Time-Series SBAS Pixel Offset Tracking Method for Monitoring Three-Dimensional Deformation in a Mining Area

JILEI HUANG[ID][1,2,3], YANG BAI[1,4], SHAOGANG LEI[3], AND KAZHONG DENG[3]

[1]Henan Industrial Technology Academy of Spatio-Temporal Big Data, Henan University, Kaifeng 475001, China
[2]College of Resources and Environment, Henan University of Economics and Law, Zhengzhou 450016, China
[3]China Ministry of Natural Resources of the People's Republic of China Key Laboratory of Land Environment and Disaster Monitoring, China University of Mining and Technology, Xuzhou 221116, China
[4]College of Environment and Planning, Henan University, Kaifeng 475001, China

Corresponding authors: Yang Bai (daisy.baiyang@henu.edu.cn) and Jilei Huang (jileihuang@126.com)

ABSTRACT The ground surface deformation caused by mining damages the ecological environment and severely hinder economic development in the mining area. The acquisition of three-dimensional ground surface deformation in a mining area helps to improve understanding of the process and mechanism of ground surface deformation caused by mining and helps to prevent and control this type of disaster. In this paper, eleven TerraSAR-X images and five Radarsat-2 images covering the 52304 working face in the Daliuta mining area were used to obtain the time-series line-of-sight (LOS) direction deformation and azimuth direction deformation based on different SAR platforms by application of the small baseline subset (SBAS) pixel offset tracking method. According to the three-dimensional solution principle of multiplatform SAR images and 72 GPS points, the accuracy of deformation in the east–west direction is 0.22 m, while the accuracy in the north–south direction is 0.21 m, with an accuracy of subsidence of 0.34 m.

INDEX TERMS SAR, pixel offset tracking, mining subsidence, three-dimensional deformation.

I. INTRODUCTION

The rapid development of China's economy is inseparable from the support of energy. Coal consumption will occupy a crucial dominant position in China's energy structure for a long time. China is both the world's largest coal consumer and the world's largest coal producer. China's statistics show that, in 2018, the raw coal production accounted for 46% of the world's total, and coal consumption accounted for 59% of China's domestic energy consumption. Over 96% of China's coal output comes from underground coal mining [1]. The large-scale extraction of underground coal will cause severe ground subsidence and horizontal displacements, severely disturbing the ground surface ecology and affecting the safety of infrastructure and public utilities [2]. Ground deformation

in coalfields has already become one of the most prominent ecological and environmental problems in China.

After the underground coal seam was mined, the internal stress balance of the surrounding rock mass was destroyed. In order to achieve a new balance, under the action of the gravity of the overlying strata in the mining area, the main movement and deformation of the rock mass occur with collapse, fracture, separation, and bending settlement. When the mining area reaches a specific range, movement and destruction will spread to the ground surface. We call the phenomenon and process of rock movement and surface deformation caused by underground coal mines mining as mining subsidence.

Mining-induced ground deformation has been studied using numerous ground-based methods, including leveling [3], total station surveys [4], and GPS field surveys [5]. These methods are not only primarily based on point-by-point

The associate editor coordinating the review of this manuscript and approving it for publication was Gerardo Di Martino[ID].

measurements but are also time-consuming, labor-intensive, and costly. To make matters worse, the workers need to enter the deformation zone to complete the survey, which significantly increases the danger. With the rapid progress in Earth observation techniques over the past several decades, the differential interferometric synthetic radar aperture (D-InSAR) and time-series InSAR methods such as PS-InSAR [6], SBAS-InSAR [2], TCP-InSAR [7] and IPTA-InSAR [8] have proven to be active within an accuracy of millimeters to centimeters along the radar line of sight (LOS) direction for mapping ground deformation induced by various natural and anthropogenic activities [9]. However, methods that are based on phase unwrapping cannot overcome the limitations of the deformation gradient and will, therefore, fail for large deformation gradients. In China, the long-wall comprehensive mechanized coal mining technique is a standard and advanced method resulting in efficient coal production and severe horizontal displacements and vertical deformation [10]. Although the time-series InSAR techniques that are based on phase unwrapping methods obtain LOS deformation with high accuracy, such techniques are usually unable to monitor the ground deformation during coal mining effectively. This is mainly due to the large ground deformation gradient caused by coal mining, which exceeds the threshold of phase unwrapping methods. In order to overcome the limitation of the surface deformation gradient and retrieve the full displacement field, long-wavelength SAR images (such as ALOS-1 and ALOS-2) are usually recommended for mining area deformation monitoring; however, the ALOS-1 satellite was discontinued in 2011, and the commercial application cost of the ALOS-2 satellite is very high [11]. The fusion of D-InSAR and sub-band InSAR [12], [13], integration of measurements from D-InSAR and TomoSAR [14] and GPS-assisted D-InSAR method [15] have been demonstrated as useful methods for monitoring ground subsidence caused by mining, but these methods are difficult to popularize. For mining monitoring accurately, applying a combination of D-InSAR and mining subsidence theory to the problem of obtaining the three-dimensional deformation of a mining area [16], [17] still faces the problem of phase unwrapping failure, restricting its use in the monitoring of large gradient deformation. Time series InSAR technology based on phase unwrapping can play a perfect role in deformation monitoring of old mined-out areas. For scenes that cause severe surface deformation during mining, time series InSAR methods based on phase unwrapping are challenging to obtain correct monitoring results due to considerable deformation gradient constraints. With improvements to the resolution of SAR images, the pixel offset tracking method based on SAR intensity information using normalized cross-correlation (NCC) has been documented as being both reliable and straightforward for measuring large-gradient surface displacements in mining areas [18]–[21]. This method can not only monitor the LOS-direction deformation but can also monitor along-track-direction displacements. For three-dimensional monitoring deformation of natural disasters, such as earthquakes,

volcanic activity, and glacier motion, which are characterized by severe damage and a wide range of spatial extents, the pixel offset tracking method has obtained satisfactory results, with the advantages of having excellent resistance to decorrelation. High-resolution three-dimensional displacements of mining areas are crucial to assessing mining-related geohazards and understanding the mining deformation mechanism [22]–[25].

The monitoring accuracy of the pixel offset tracking method mainly depends on the pixel size of the SAR image. The local surface deformation caused by coal mining has a large deformation gradient and a small influence range. To accurately obtain the 3D deformation of the mining area, high-resolution SAR images are essential.

In recent years, the pixel offset tracking method has made significant progress in monitoring the three-dimensional deformation of mining areas. In summary, there are two types of methods: 1. Multi-platform SAR image fusion monitoring; 2. SAR image pixel offset tracking + mining subsidence model. The multi-platform SAR image fusion monitoring method can theoretically accurately monitor the three-dimensional deformation of the mining area. However, due to the limited number and resolution of satellites in orbit, the research area has difficulty meeting the requirements. Researchers found that SAR pixel offset tracking + mining subsidence model methods can achieve ideal monitoring results. For example, Yang *et al.* [26]–[30] proposed a method for retrieving 3D deformation from a single SAR amplitude pair (SAP) with the assistance of a prior mining deformation model and Chen [31] revealed 3D varying large surface displacements in Daliuta Mining Area through the integration of the SAR pixel offset tracking and mining subsidence model. However, these methods rely on the choice of mining subsidence model and parameters and are not suitable for mountainous areas or highly inclined coal seams.

In this paper, a novel time-series pixel offset tracking method based on the integration of TerraSAR-X SAR images in descending orbit and Radarsat-2 SAR images in ascending orbit are used to reveal the large-gradient three-dimensional ground surface deformation caused by mining in the Daliuta Mining Area. According to the validation of 72 GPS monitoring points along the strike direction and dip direction above the working face in the mine, this method is useful for monitoring large-gradient three-dimensional ground surface deformation.

II. METHODOLOGY
A. TIME SERIES SBAS PIXEL OFFSET TRACKING METHOD
The pixel offset tracking method based on SAR intensity information uses the NCC of the input SAR intensity images to estimate the slant- and along-track-direction deformations. The most significant advantage of the pixel offset tracking method based on SAR intensity information is influenced very little by temporal and spatial coherence and deformation gradients. However, if the temporal baseline and spatial baseline are both substantial, this will reduce monitoring

accuracy and possibly even failure. The capability of the SBAS-DInSAR technique which relies on an appropriate selection of the SAR image pairs characterized by a small spatial and temporal separation (baseline) between the acquisition orbits, thereby reducing some of the more problematic noise sources in interferometry to accurately measure displacements has already been well documented in case studies [32]. In this paper, an extension of the pixel offset tracking SBAS techniques has been proposed to move from the investigation of large-gradient mining deformations toward temporally varying phenomena. Generally, the pixel offset tracking method obtains the surface deformation with an accuracy of 1/10-1/20 pixel size. Therefore, high-resolution SAR images guarantee the ability to obtain stable monitoring results. This approach follows the same rationale as the conventional SBAS-DInSAR technique and is expressed as follows:

$$B\boldsymbol{\varphi} = D_{los} \qquad (1)$$

where B is an $M \times N$ coefficients matrix with M representing the selected pixel tracking pairs and N representing the number of SAR images; $\boldsymbol{\varphi}$ is the unknown vector representing the deformations between time-adjacent SAR acquisitions (unknown terms); and D_{los} represents the monitoring deformation vector obtained by the pixel offset tracking (known terms). For the SBAS pixel offset tracking approach, the constraints of the temporal and spatial baselines are less stringent than those of the conventional SBAS-DInSAR technique based on phase unwrapping. In general, B is an N-rank matrix and its solution can be obtained according to the least squares principle as:

$$\hat{\boldsymbol{\varphi}} = B^{\#} D_{los} \qquad (2)$$

with $B^{\#} = (B^T B)^{-1} B^T$.

Unfortunately, if B exhibits a rank deficiency, then singular value decomposition (SVD) is required to obtain the optimal solution.

B. 3D DEFORMATION FROM SBAS PIXEL OFFSET TRACKING METHOD

In recent decades, considerable effort has been made to resolve the full three-dimensional displacements from the multiple D-InSAR measurements. Generally, by exploiting the multiple D-InSAR measurements acquired from at least three imaging geometries, the three-dimensional displacement can be acquired with the following equations:

$$\begin{bmatrix} d_u \\ d_e \\ d_n \end{bmatrix} = \boldsymbol{\Gamma} \cdot \begin{bmatrix} d_{los,1} \\ d_{los,2} \\ d_{los,3} \end{bmatrix} \qquad (3)$$

with

$$\boldsymbol{\Gamma} = \begin{bmatrix} a_1 & b_1 & c_1 \\ a_2 & b_2 & c_2 \\ a_3 & b_3 & c_3 \end{bmatrix}^{-1}; \quad a_i = \cos\theta_{inc,i}, \ i = 1, 2, 3;$$

$$b_i = -\sin\theta_{inc,i}\sin\left(\alpha_{az,i} - 3\pi/2\right), \quad i = 1, 2, 3;$$

$$c_i = -\sin\theta_{inc,i}\cos\left(\alpha_{az,i} - 3\pi/2\right), \quad i = 1, 2, 3$$

where d_u, d_e, and d_n are the deformation in three directions; and $d_{los,1}$, $d_{los,2}$, and $d_{los,3}$ are the three InSAR LOS measurements. $\theta_{inc,i}$ and $\alpha_{az,i}$ are the radar incidence angle and the orbit azimuth angle (positive clockwise from north), respectively, for the ith InSAR LOS measurement.

For the pixel offset tracking method, not only can the deformations in the LOS direction be monitored, but along-track-direction deformations can also be acquired. According to the pixel offset tracking method, only two SAR imaging geometries are sufficient to resolve complete three-dimensional displacement with the following equations:

$$\begin{cases} d_{los,1} = d_u \cos\theta_{inc,1} - \sin\theta_{inc,1}\cos\alpha_{az,1}d_e \\ \qquad + \sin\theta_{inc,1}\sin\alpha_{az,1}d_n \\ d_{los,2} = d_u \cos\theta_{inc,2} - \sin\theta_{inc,2}\cos\alpha_{az,2}d_e \\ \qquad + \sin\theta_{inc,2}\sin\alpha_{az,2}d_n \end{cases} \qquad (4)$$

And

$$d_{az} = -d_e \cos\left(\alpha - \frac{3\pi}{2}\right) + d_n \sin\left(\alpha - \frac{3\pi}{2}\right)$$

$$\begin{bmatrix} d_u \\ d_e \end{bmatrix} = \mathbf{A}^{-1} \cdot \mathbf{B}, \ d_n = \frac{d_{az} - d_e \sin\alpha}{\cos\alpha} \qquad (5)$$

With

$$\mathbf{A} = \begin{bmatrix} \cos\theta_{inc,1} & -\sin\theta_{inc,1}(\cos\alpha_{az,1} + \tan\alpha_{az,1} \cdot \sin\alpha_{az,1}) \\ \cos\theta_{inc,2} & -\sin\theta_{inc,2}(\cos\alpha_{az,2} + \tan\alpha_{az,2} \cdot \sin\alpha_{az,2}) \end{bmatrix},$$

$$\mathbf{B} = \begin{bmatrix} d_{los,1} - \sin\theta_{inc,1}\tan\alpha_{az,1}d_{az,1} \\ d_{los,2} - \sin\theta_{inc,2}\tan\alpha_{az,2}d_{az,2} \end{bmatrix}$$

where $d_{los,1}$ and $d_{los,2}$ are the measured deformations in the LOS direction from different SAR images using the SBAS pixel offset tracking method; $d_{az,1}$ and $d_{az,2}$ are the measured deformations in the along-track direction from two different SAR images obtained by the SBAS pixel offset tracking method; $\theta_{inc,1}$ and $\theta_{inc,2}$ are the radar incidence angles according to different SAR image geometries; and $\alpha_{az,1}$ and $\alpha_{az,2}$ are the different orbit azimuth angles.

III. STUDY AREA AND DATA PROCESSING
A. STUDY AREA AND DATA
The study area is located in Shenmu county, north of Yulin city, in Shaanxi province. The Daliuta coal mine is one of the largest coal mines in China. It is located in the Mu Us Desert foothills region at high elevations ranging from 901 meters to 1331 meters. The climate is characterized by dry, long winters with frequent sandstorms, and little snow or rain, and by short summers. Due to the long-term coal mining, the ecological environment in this area is fragile. There are two working faces in this study area, 52304 and 22307, as shown in Figure 1.
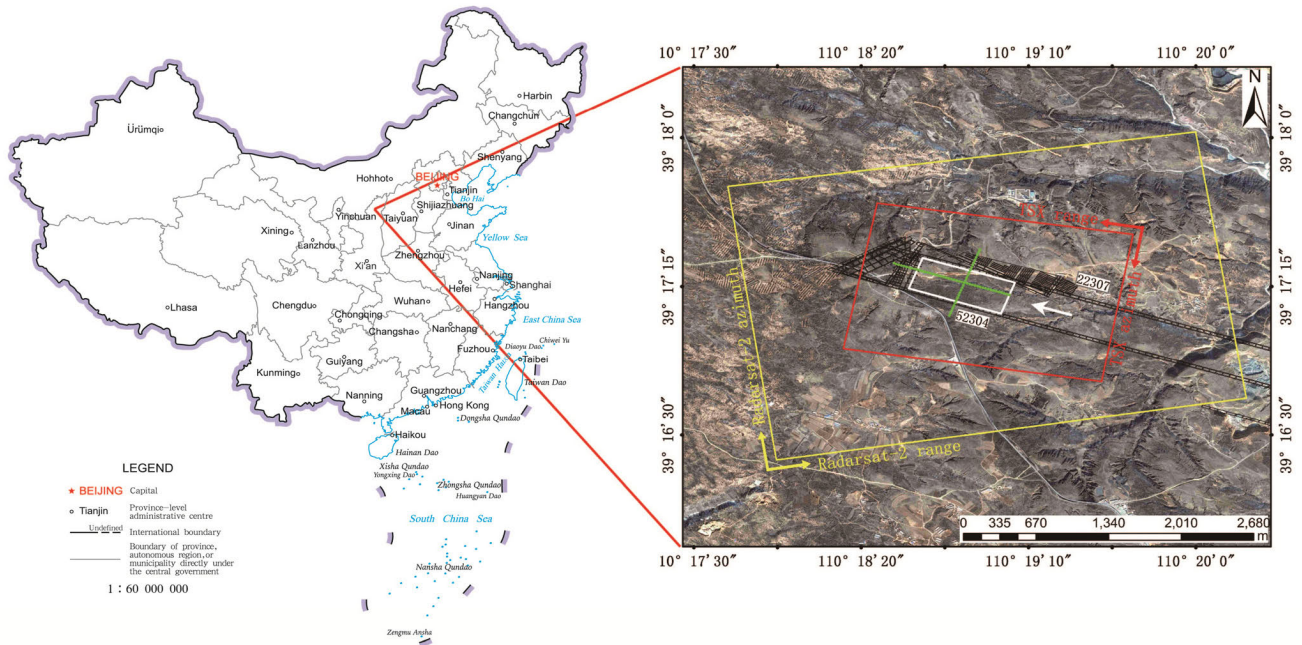
FIGURE 1. Study area location. The red frame represents the coverage of TerraSAR-X (TSX); the yellow frame represents the coverage of Radarsat-2; the white frame represents the 52304 working face; the white arrow represents the mining direction; and the green points represent GPS points.

TABLE 1. TerraSAR-X and Radarsat-2SAR image parameters.

Satellite	Imaging mode	Pixel size (m)	Heading angle(°)	Revisit time (days)	Number of images
TerraSAR-X	spotlight	0.86*0.98	-170.502	11	11
Radarsat-2	stripmap	2.66*2.88	-8.725	24	5

The working face 22307 was entirely exhausted by the room-and-pillar method in 2005, and the residual ground subsidence was very small. Considering the individual mining processes of working face 22307, it made little contribution to the ground subsidence that the five Radarsat-2 SAR images captured in ascending orbit and eleven TerraSAR-X SAR images in descending orbit. The Radarsat-2 SAR images, with a pixel spacing of 2.66 m in the slant range and 2.88 m in azimuth, and TerraSAR-X spotlight images, with a pixel spacing of 0.86 m in the slant range and 0.98 m in azimuth, are used to monitor mining deformations by the application of the time-series SBAS pixel offset tracking method. The SAR image information is shown in detail in Table 1. Because the fully mechanized caving technique was used on working face 52304, the subsidence rate and spatial extent of this working face were both large. The mining conditions of working face 52304 were as follows: the elevation of the ground surface was from 1154.8 meters to 1269.9 meters, the mining depth was 235 m, and the average thickness of the coal seam was 6.94 m. A total of 45 GPS survey points in the strike direction and 27 in the dip direction, monitored on Nov 21th, 2012,

and Apr 1st, 2013, were used to test the accuracy of the time-series SBAS pixel offset tracking method in monitoring three-dimensional deformations caused by mining.

B. DATA PROCESSING

When the pixel sizes of the SAR images of the two platforms are close, the above method (shown in part II.B) can restore the three-dimensional deformation. When the pixel sizes of the SAR images of the two platforms are quite different, the above method will reduce the accuracy of the three-dimensional calculation, and even lead to the failure of the recovery of the deformation field. For the pixel offset tracking method, a larger pixel size means lower monitoring accuracy. In the study area of this paper, the azimuthal deformation is significantly smaller than the sinking. The Radarsat-2 images with pixel sizes of 2.66*2.88 m can effectively capture the line of sight sinking information, and it is not easy to obtain the azimuth deformation correctly. Since the Radarsat-2 image's pixel size is almost three times that of the TerraSAR-X image, we use the high-resolution TerraSAR-X images to resolve the north-south deformation
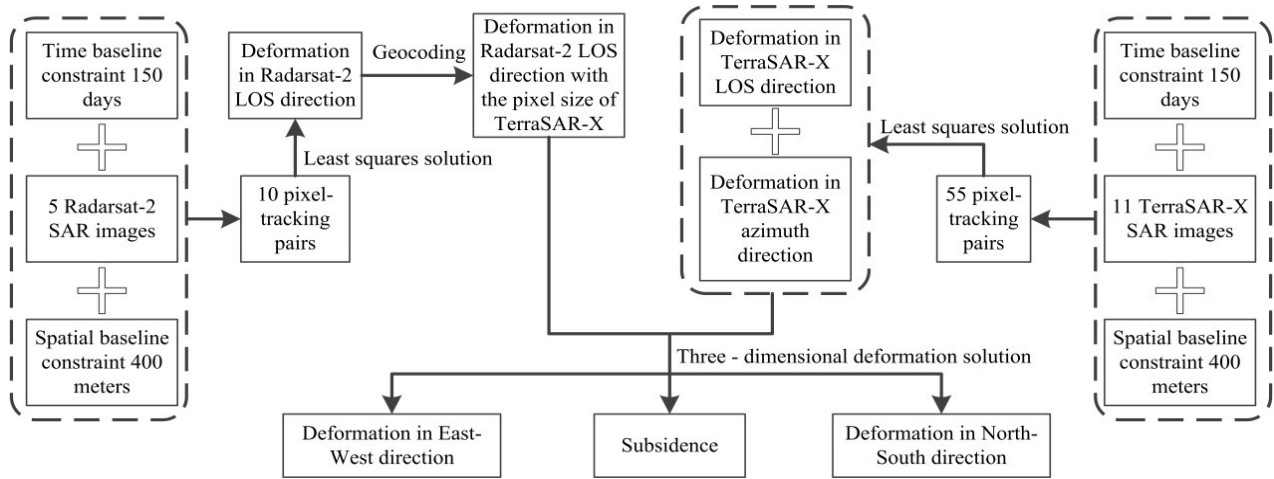
FIGURE 2. The process flow of the time-series SBAS pixel offset tracking method.
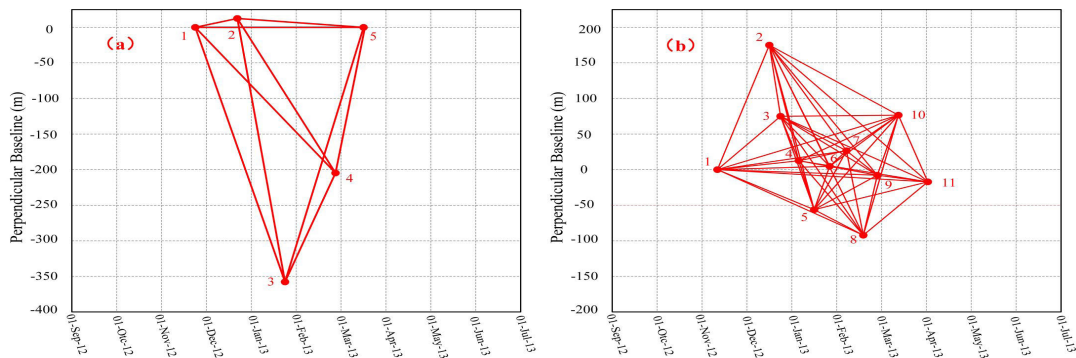

FIGURE 3. The relationship between temporal baseline and the spatial baseline. (a) for Radarsat-2; (b) for TerraSAR-X.

approximation instead of the north-south deformation of the Radarsat-2 images at the same time. The formula is as follows:

$$
\begin{cases}
d_{los,TX} - d_{az,TX} \sin\theta_{inc,TX} \tan\alpha_{az,TX} = d_u \cos\theta_{inc,TX} \\
\quad - \sin\theta_{inc,TX}(\cos\alpha_{az,TX} + \tan\alpha_{az,TX}\sin\alpha_{az,TX})d_e \\
d_{los,R2} - d_{az,TX}\dfrac{\sin\theta_{inc,R2}\sin\alpha_{az,R2}}{\cos\alpha_{az,TX}} = d_u\cos\theta_{inc,R2} \\
\quad - \sin\theta_{inc,R2}(\cos\alpha_{az,R2} + \tan\alpha_{az,TX}\sin\alpha_{az,R2})d_e
\end{cases}
\tag{6}
$$

where $d_{los,TX}$, $d_{los,R2}$ are the LOS measurements of TerraSAR-X and Radarsat-2, $\theta_{inc,TX}$, $\theta_{inc,R2}$ and $\alpha_{az,TX}$, $\alpha_{az,R2}$ are the radar incidence angle and the orbit azimuth angle of TerraSAR-X and Radarsat-2, $d_{az,TX}$ is the measured deformations in the along-track direction of TerraSAR-X.

Typically, different SAR platforms correspond to different SAR image pixel sizes. In order to combine the multi-platform SAR images by the SBAS pixel offset tracking method for three-dimensional deformations, the multi-platform SAR image pixel sizes must be unified. A geocoding method is used to unify the pixel sizes and to ensure the successful recovery of three-dimensional deformations caused

by mining. The process flow of the whole algorithm is shown in Figure 2.

IV. RESULTS AND DISCUSSION

A. RESULTS OF TIME-SERIES SBAS PIXEL OFFSET TRACKING

The pixel offset tracking method has less constraint on the time baseline and the spatial baseline than the phase unwrapping method. A temporal baseline constraint of 150 days and a spatial baseline constraint of 400 meters are appropriate, and 55 pixel-tracking pairs for eleven TerraSAR-X images and 10 pixel-tracking pairs for five Radarsat-2 images are generated, respectively, in order to reveal the time series deformations caused by mining. The relationship between the time baseline and the spatial baseline for TerraSAR-X and Radarsat-2 is shown in Figure 3.

As shown in Figure 4, ten time-series deformation images in the TerraSAR-X LOS direction from Nov. 10th, 2012, to Apr. 2nd, 2013, display the ground surface deformation processes arising from coal mining. With the forward motion of the development of the mining working face, the scope and magnitude of surface subsidence gradually expanded, and the
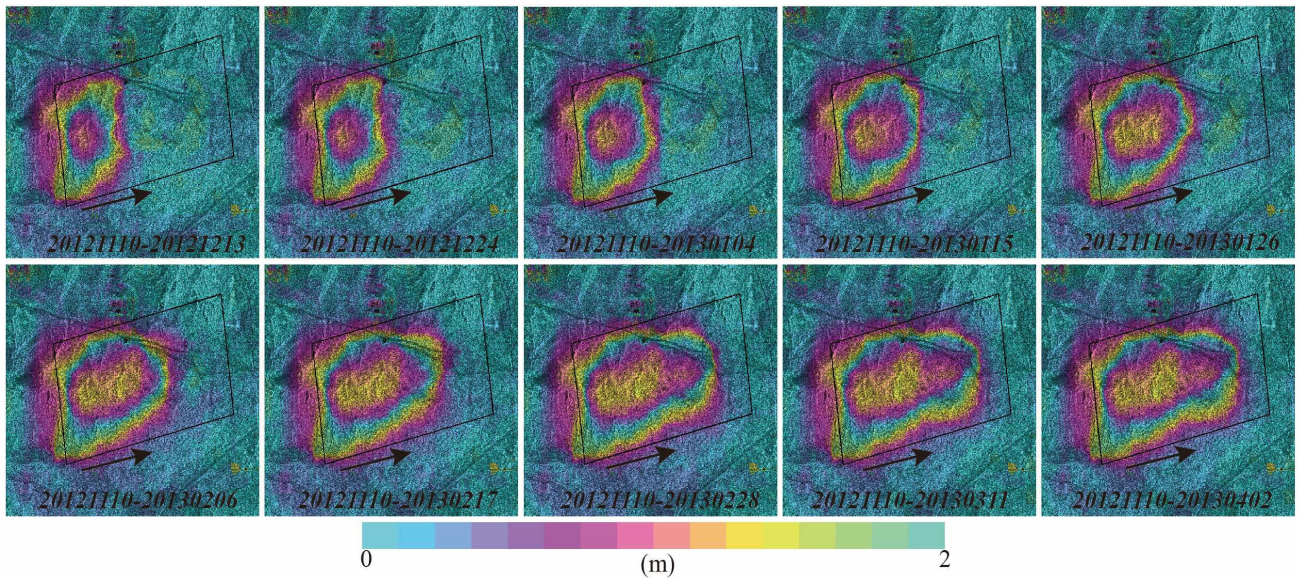
FIGURE 4. Time-series deformation images in the TerraSAR-X LOS direction. The black frame represents the 52304 working face; the black arrow represents the mining direction in TerraSAR-X geometry. The positive values represent movement along the LOS direction.
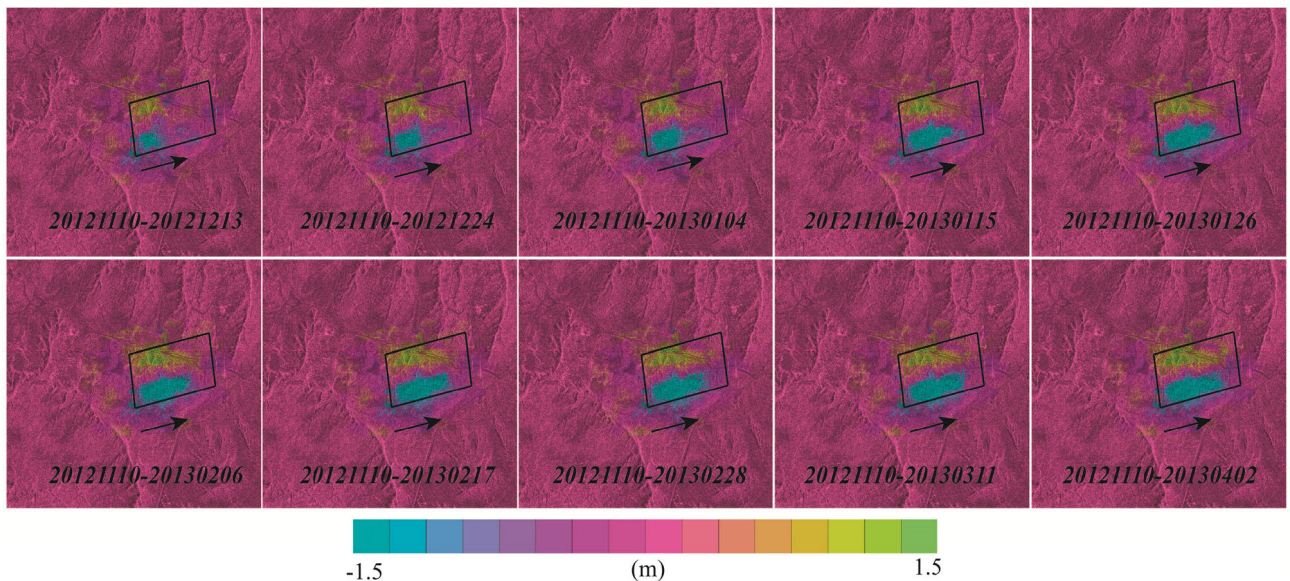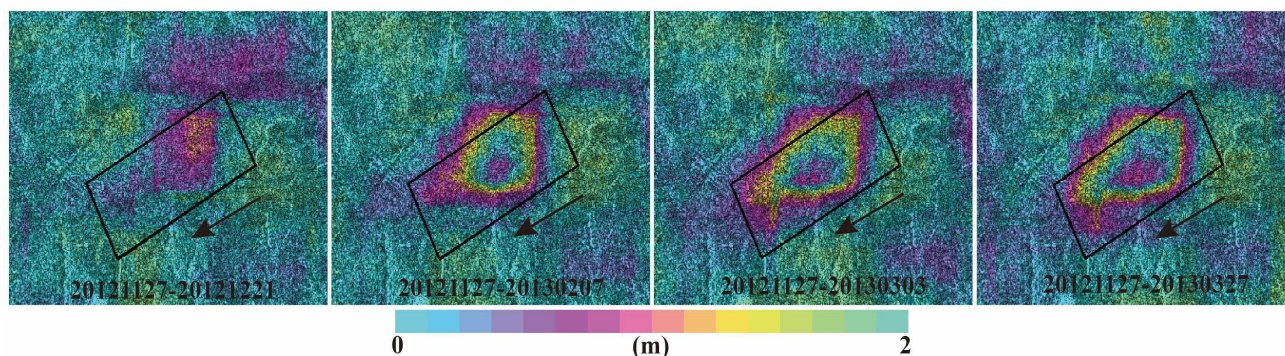

FIGURE 5. Time-series deformation images in the TerraSAR-X azimuth direction. The black frame represents the 52304 working face; the black arrow represents the mining direction in TerraSAR-X geometry. The positive values represent movement along the TerraSAR-X azimuth direction.

center of the subsidence basin gradually expanded along the mining direction.

Figure 5 shows the process of 52304 working face deformation along the azimuth of TerraSAR-X image during mining. With the excavation of the mining, the azimuthal deformation from the TerraSAR-X images shows two distinct features in the time series. The first is that with the development of the mining, the azimuth deformation moves toward the center line of the 52304 working face; the second is that the influence range of the azimuth deformation gradually expands, with the excavation of the mining, when

approaching the end of the 52304 working face, the azimuthal deformation is significantly reduced.

Figure 6 shows four time-series deformation images in the Radarsat-2 LOS direction from Nov. 27th, 2012, to Mar. 27th, 2013. The shape of the subsidence basin shown in Figure 6 is significantly different from that in Figure 4. This is mainly caused by two factors. One factor is that, due to the different observation periods, the ground surface shows different subsidence characteristics. A second factor is that two types of SAR images from different satellite platforms were used: one type was TerraSAR-X images in descending orbit, with

FIGURE 6. Time-series deformation images in the Radarsat-2 LOS direction. The black frame represents the 52304 working face; the black arrow represents the mining direction in Radarsat-2 geometry. The positive values represent movement along the LOS direction.
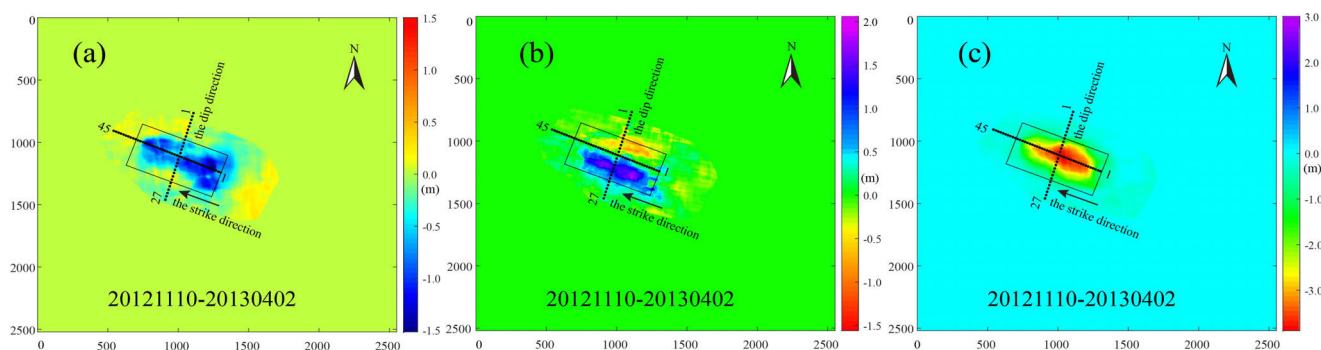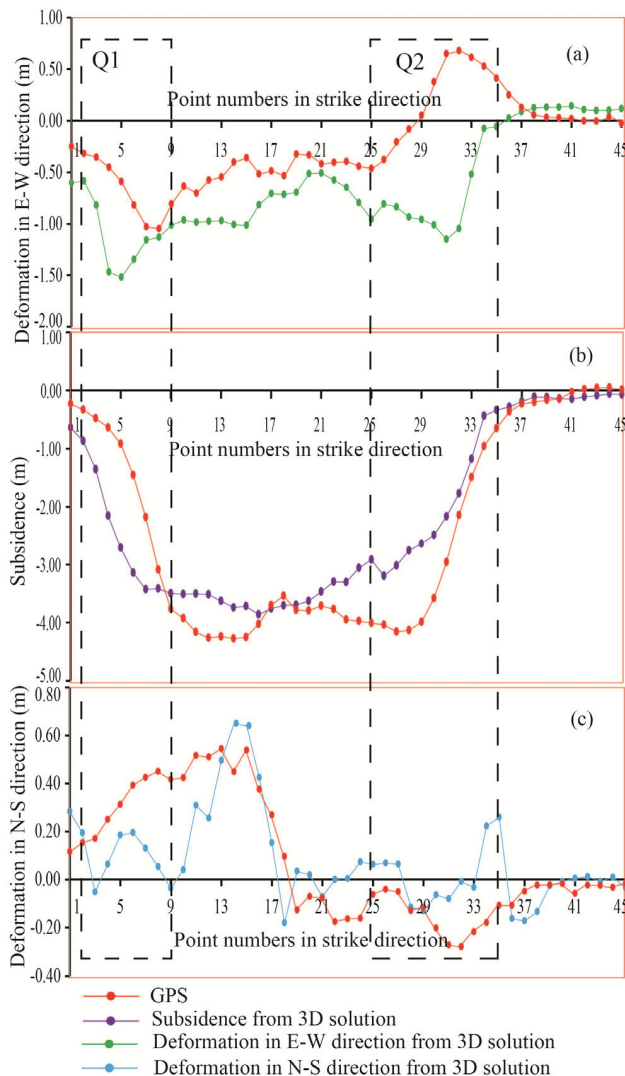

FIGURE 7. Three-dimensional deformation. (a) East–west direction deformation; (b) North–south direction deformation; (c) Subsidence of the mining area. The black frame represents the 52304 working face; the black arrow represents the mining direction; the black points represent GPS monitoring points with 45 in the strike direction and 27 in the dip direction. The positive values represent uplift, eastward movement, and northward movement, respectively.

a pixel spacing of 0.86 m in the slant range and 0.98 m in azimuth, and the other was Radarsat-2 images in ascending orbit, with a pixel spacing of 2.66 m in the slant range and 2.88 m in azimuth. Although the ground surface subsidence exhibits different shapes in the two different SAR geometries, both types of SAR images are able to accurately capture the appearance of the ground surface subsidence caused by mining.
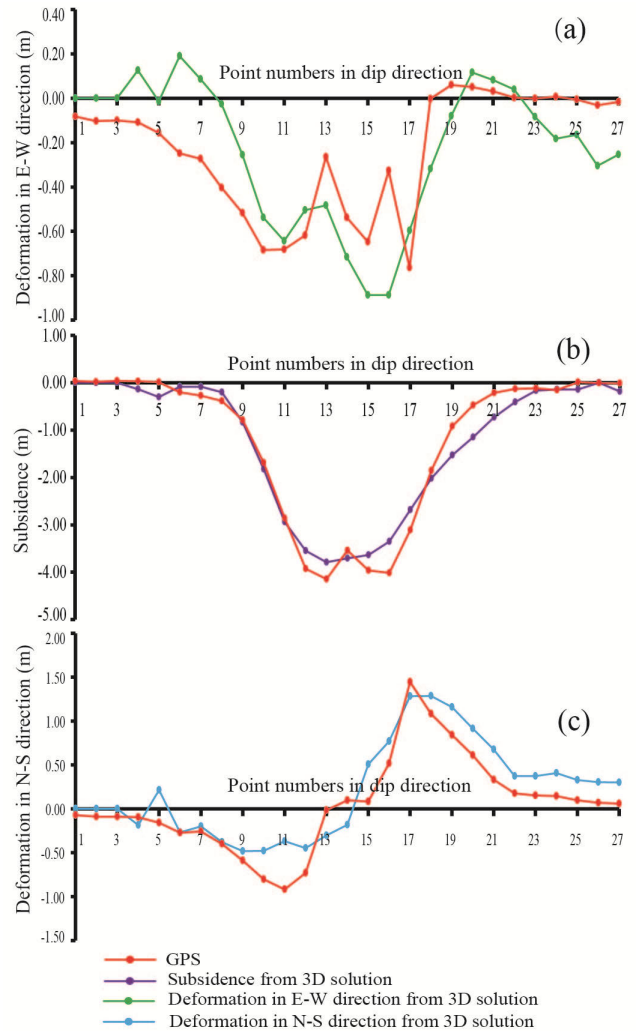
B. RESULTS OF 3D DEFORMATION

Coal mining-induced ground surface deformation, in the case of full mining (not only subsidence), is associated with a horizontal movement in the east–west and north–south directions. In this paper, eleven TerraSAR-X images and five Radarsat-2 images are used to obtain the deformation in different LOS directions by the time-series SBAS pixel offset tracking technique, and the 3D deformation of the mining area is obtained by the method described in Section III. B. Additionally, 45 GPS points in the strike direction and 27 GPS points in the dip direction, monitored on Nov. 21th, 2012, and Apr. 1st, 2013, was used to test the accuracy of the 3D deformation.

Figure 7(a) shows the east–west-direction deformation; it was found that the east–west-direction deformation occurred in most of the mining area and to the west. According to the validation provided by 45 GPS points in the strike direction (shown in Figure 8(a)), it was found that in the areas of Q1 and Q2 the error between the 3D solution results and the GPS results is large. This is mainly because the different platforms' SAR images monitoring times are not uniform. In Q1, the absolute values of 3D solution results are more significant than the GPS results; this is due to the TerraSAR-X images being acquired from Nov. 10th, 2012, to Apr. 2nd, 2013, whereas the GPS points were monitored on Nov. 21th, 2012. From Nov. 10th to Nov. 21th, the deformation was captured by TerraSAR-X images, but the GPS results were not captured. In Q2 areas, the east–west-direction deformation from the 3D solution is obviously different from the GPS points. This is due to the fact that the Radarsat-2 images were acquired from Nov. 27th, 2012, to Mar. 27th, 2013. From Mar. 27th, 2013, to Apr. 2nd, 2013, the deformation was only captured by TerraSAR-X images, and, during this period, severe deformation of the ground surface was continuing, resulting in errors in the 3D solution. Without considering Q1 and Q2, the mean absolute difference value (MADV)

FIGURE 8. Comparison between GPS and the three-dimensional solution in the strike direction. (a) East–west direction deformation; (b) Subsidence. (c) North–south direction deformation. Two black dashed boxes labeled Q1 and Q2 represent areas with large MADV.

FIGURE 9. Comparison between the GPS and three-dimensional solutions in the dip direction. (a) East–west direction deformation; (b) Subsidence. (c) North–south direction deformation.
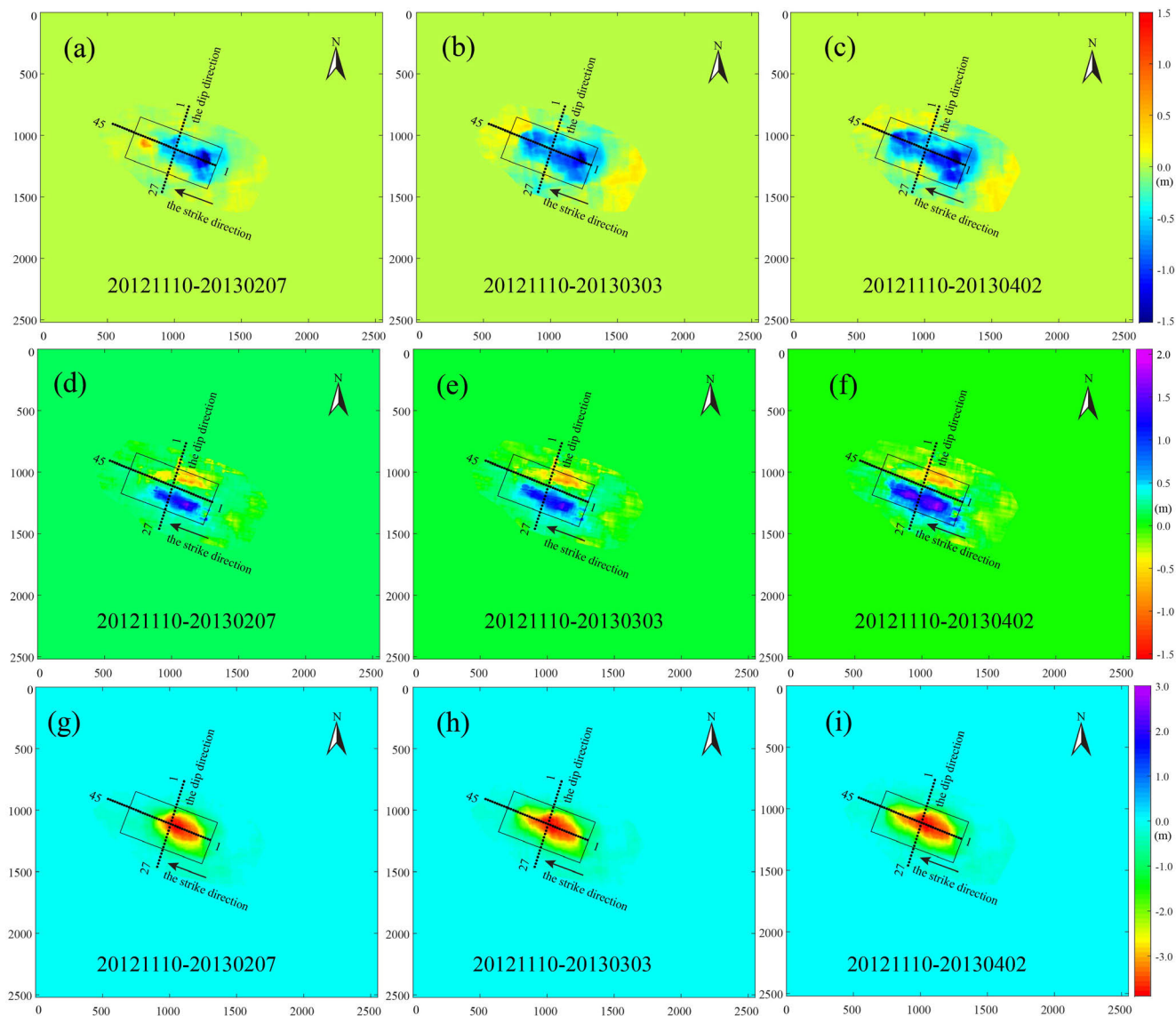
between the east–west-direction deformation from the 3D solution and the GPS results in the strike direction is 0.24 m, and the Root Mean Square Error (RMSE) is 0.29 m. As shown in Fig. 9 (a), 27 GPS monitoring points in the dip direction are used to verify the accuracy of the deformation in the east-west direction, and the monitoring results are better than that in the strike direction. Along the dip line, the MADV between the east–west direction deformation from the 3D solution and the GPS results is 0.19m, and RMSE is 0.23m. This is mainly because the GPS monitoring stations along the dip line are located in the middle of the 52304 working face. When the deformation occurs, it is easy to be captured by TerraSAR-X and Radarsat-2 images at the same time, which has good consistency of observation time. Using the monitoring data of the GPS monitoring stations of the strike direction and dip direction to evaluate the accuracy in the east-west direction as a whole, the MADV is 0.26m, and the RMSE is 0.22m.

Figure 7(b) shows the north–south direction deformation. The deformation in the north–south direction shows a tendency to move toward the center, with the strike direction observation line of the working face as the boundary. The north–south direction deformation from pixel offset tracking coincided well with the 27 GPS observations in the dip direction (shown in Figure 9(c)), with a MADV of 0.22 m and an RMSE of 0.25 m. According to the monitoring data of 45 GPS monitoring stations in the strike direction, the deformation in the direction of "North- South " also occurred. Figure 8 (c) shows a comparison between GPS and the three-dimensional solution in the "South-North" direction of the 45 GPS monitoring stations along the strike direction. In the Q1 and Q2 regions, the consistency between the two is poor, which is still caused by the inconsistency at the observation time. Without considering the monitoring stations in the Q1 and Q2 areas, the MADV between the North–South direction deformation from the 3D solution and the GPS results in the strike direction is 0.12m, and the RMSE is 0.16m.

FIGURE 10. Time series three-dimensional deformation. (a), (b), (c) East–west-direction deformation in time series; (d), (e), (f) North–south-direction deformation in time series; (g), (h), (i) Subsidence of the mining area in time series. The positive values represent uplift, eastward movement, and northward movement, respectively.

The deformation monitoring accuracy of the '' North- South '' direction (without Q1 and Q2) along the strike direction is better than that of the dip direction. This is mainly due to the small deformation in the ''south-north'' direction along the strike direction. Accuracy evaluation is carried out using GPS monitoring stations along the strike direction (without Q1 and Q2), and the dip direction, the MADV between the north–south direction deformation from the 3D solution and the GPS results is 0.17m, and the RMSE is 0.21m.

Figure 7(c) shows the subsidence in the mining area. Figure 8(b) and Figure 9(b) illustrate the comparison between the subsidence of the 3D solution and the GPS results in strike and dip directions, respectively. In the dip direction, the subsidence of the 3D solution coincided well with the 27 GPS observations. However, in the strike direction, the subsidence

of the 3D solution coincided poorly with GPS observations in Q1 (where the subsidence of the 3D solution is larger than that of GPS data) and in Q2 (where the subsidence of the 3D solution is smaller than that of GPS data). This is mainly due to the monitoring times of TerraSAR-X and Radarsat-2 and GPS not being uniform. Without considering Q1 and Q2, the MADV between the subsidence of the 3D solution and GPS results is 0.26 m, with an RMSE of 0.34 m.

To reveal the dynamic change process of surface deformation caused by coal mining, TerraSAR-X images and Radarsat-2 images captured at similar times were selected and processed by the time-series SBAS pixel offset tracking method, and the results are shown in Figure 10. With the advance of the mining working face, the influence range and

magnitude of east-west deformation gradually increase, and visible deformation appears above the collapse position of coal seam roof (shown in Figure 10(a), 10(b), 10(c)). The north-south deformation caused by coal mining is associated with relative movement in the working face toward the Central Line (shown in Figure 10(d), 10(e), 10(f)). As the working face advances, the sinking center moves along the strike direction (shown in Figure 10(g), 10(h), 10(i)). Time series monitoring results show that the deformation near the starting line of the mining face is significantly larger than that near the stop-mining line. This is because, during the image coverage period, underground mining-out activities were taking place, and the surface deformation caused by mining was active and had not stabilized. The severe surface deformation caused by coal mining is a serious disaster. In order to ensure the safety of the monitors, no ground GPS survey was carried out during the mining process. Therefore, accuracy verification of the monitoring results during the mining process cannot be carried out.

For the 52304 working face in Daliuta mining area, some researchers have obtained better results by using the method of pixel offset tracking combined mining subsidence model. For example, Yang used the single amplitude pair of SAR using the offset tracking combined mining subsidence model method to obtain the three-dimensional surface deformation of the study area [26]. In the time series, Yang acquired the three-dimensional surface deformation in two periods from November 21, 2012 to February 6, 2013 and November 21, 2012 to April 2, 2013. Compared with the results of this paper from November 21, 2012 to February 7, 2013, in the sinking and north-south directions, the deformation trends of the two agree well in time series. In the east-west direction, the trend of deformation between the two is basically the same, but in quantitative analysis, it is difficult to evaluate which result is more objective, because of the lack of in-site GPS verification data during this period. Comparing the three-dimensional deformation between November 21, 2012 and April 2, 2013, it also shows that the two have a high consistency of the deformation trend in the sinking and north-south directions, and a weak consistency in the deformation trend in the east-west direction. Fortunately, there are in-site GPS measurement data that can be used for objective accuracy evaluation during this period. In Yang's research, only 26 GPS observation stations along the dip direction in 52304 working face were used to assess accuracy from two aspects: sinking and horizontal movement. In order to ensure the objectivity of the comparison, this paper also adopts the same GPS monitoring stations to evaluate the accuracy from sinking and horizontal movement. According to Yang's research, the RMSE is 0.227m in the sinking direction and 0.415m in the horizontal direction. The RMSE using the method proposed in this paper is 0.29m in the sinking direction and 0.25m in the horizontal direction. Subsequently, Yang proposed an improved method to monitor this area and verified it with 26 GPS data. The sinking accuracy was 0.17 m, and the horizontal movement accuracy was 0.14 m [30].

Chen used the integration of SAR pixel offset tracking and mining subsidence model combined support vector regression algorithm to restore the three-dimensional deformation of this area, and verified the data from a total of 71 GPS observation stations. The RMSE yielded better monitoring results. The movements in the vertical, east-west, and north-south directions were 12.4 cm, 13.1 cm, and 14.4 cm, respectively [31]. For the time-series deformation of the 52304 during mining, the time period shown in this paper is different from the time period shown in Chen's research. However, the consistency of the deformation trend of the two in sinking and north-south directions is very well, and the consistency of the deformation trend in the east-west direction is weak.

By comparing the three-dimensional time series deformation monitoring results of Yang's and Chen's, it is also shown that the consistency of the deformation trend in the sinking and north-south directions is excellent, and the consistency of the deformation trend in the east-west direction is little weak. The weak consistency of the east-west deformation trend may be due to the close relationship between the east-west deformation and the removal of hydraulic support during coal mining. For the working face that meets the full mining conditions, with the mining excavation, the center position of the working face usually reciprocates in the east-west direction. Therefore, at different observation times, the deformation in the east-west direction may be significantly different.

The monitoring accuracy of the method proposed in this paper is close to that of Yang's, but it is worse than that of Chen's. This is mainly because the pixel size of the Radarsat-2 image in the method used in this paper is almost three times that of the TerraSAR-X image (although they are all high-resolution images), which causes the monitoring accuracy of the Radarsat-2 image is low. Therefore, when the joint solution is performed, the overall monitoring accuracy is reduced. On the other hand, the inconsistency of the satellite observation time brings some errors to the solution of the three-dimensional monitoring results.

The method of pixel offset tracking + mining subsidence model can achieve ideal monitoring results in this area mainly due to two aspects: 1. The use of high-resolution TerraSAR-X images can obtain monitoring results using the ideal pixel offset tracking method, 2. The coal seam inclination angle of the mining working face 52304 is almost horizontal, and the geological conditions in this area are simple. The coal seam is shallow, which is very suitable for the application of the mining subsidence model.

After underground coal is mined, the original stress equilibrium state of the overlying rock above the coal seam to the surface is disturbed. In the process of reaching the new stress equilibrium state, the surface will sink and move horizontally (in the east-west and north-south directions). Using new observation methods (such as TS-InSAR and time-series pixel offset tracking) to carry out time-series surface 3D deformation monitoring of the mining area is of great significance for better understanding and development of the mining subsidence mechanism, helping the mining area to

carry out ecological restoration and allowing the mining area to produce safely.

The advantage of the method proposed in this paper to monitor the time-series three-dimensional deformation of the mining area is that this method is not restricted by mining subsidence models and parameters, and is suitable for surface deformation monitoring in various scenarios (such as steeply inclined coal seams and mountain areas). At present, there are mainly two factors restricting this method. One is that the large pixel size of the SAR image leads to a low monitoring accuracy of the pixel-tracking method. The other is that, due to the small number of SAR satellites in orbit, it is difficult to ensure the consistency of the same target observation time. As more and more advanced SAR satellites are launched in the future, these problems should be significantly improved.

V. CONCLUSION
In this paper, a method of time-series SBAS pixel offset tracking based on multi-platform SAR images is proposed to determine the 3D deformation in a mining area. Eleven TerraSAR-X images and five Radarsat-2 images are used to reveal the temporal and spatial process of ground surface deformation caused by mining in the LOS direction and azimuth direction. According to the 3D solution and 72 GPS results, the MADV is 0.26 m with an RMSE of 0.22 m in the east–west direction, while the MADV is 0.17 m with an RMSE of 0.21 m in the north–south direction. The MADV and RMSE of the subsidence are 0.26 m and 0.34 m, respectively. Although the monitoring accuracy of this method is not as high as traditional measurements, the acquisition of the time series three-dimensional deformation of the mining area helps to improve the understanding of the mechanism and process of ground surface deformation caused by mining. By comparing the research of Yang's and Chen's, it can be seen that the pixel offset tracking method based on high-resolution SAR images combined with the mining subsidence model can obtain more accurate 3D deformation information. However, it is usually necessary to satisfy the working face's geological conditions better to meet the assumptions of the mining subsidence theoretical model. Due to the significant difference in the pixel size of SAR images on different platforms, the monitoring accuracy of the method adopted in this paper is low. Therefore, in the future research work, we should focus on how to improve the monitoring accuracy of the 3D solution of time-series SBAS pixel offset tracking and how to evaluate the overall accuracy.

REFERENCES

[1] L. Jia-ming, Y. Jian-hui, and Z. Wen-zhong, "Spatial distribution and governance of coal-mine subsidence in China," *J. Natural Resour.*, vol. 34, no. 4, pp. 867–880, 2019.

[2] L. Jiang, H. Lin, J. Ma, B. Kong, and Y. Wang, "Potential of small-baseline SAR interferometry for monitoring land subsidence related to underground coal fires: Wuda (Northern China) case study," *Remote Sens. Environ.*, vol. 115, no. 2, pp. 257–268, Feb. 2011, doi: 10.1016/j.rse.2010.08.008.

[3] D. Raucoules, C. Carnec, S. Le Mouelic, C. King, and C. Maisons, "Comparison between InSAR and leveling," in *Proc. IEEE Int. Geosci. Remote Sens. Symp. (IGARSS)*, vol. 4, Jul. 2003, pp. 2939–2941.

[4] A. H.-M. Ng, L. Ge, and X. Li, "Assessments of land subsidence in the Gippsland basin of Australia using ALOS PALSAR data," *Remote Sens. Environ.*, vol. 159, pp. 86–101, Mar. 2015.

[5] J. Wang, X. Peng, and C. H. Xu, "Coal mining GPS subsidence monitoring technology and its application," *Mining Sci. Technol. (China)*, vol. 21, no. 4, pp. 463–467, Jul. 2011.

[6] S. Abdikan, M. Arıkan, F. B. Sanli, and Z. Cakir, "Monitoring of coal mining subsidence in peri-urban area of Zonguldak city (NW Turkey) with persistent scatterer interferometry using ALOS-PALSAR," *Environ. Earth Sci.*, vol. 71, no. 9, pp. 4081–4089, May 2014.

[7] L. Lu, H. Fan, J. Liu, J. Liu, and J. Yin, "Time series mining subsidence monitoring with temporarily coherent points interferometry synthetic aperture radar: A case study in Peixian, China," *Environ. Earth Sci.*, vol. 78, no. 15, p. 461, Aug. 2019.

[8] P. Teatini, T. Strozzi, L. Tosi, U. Wegmüller, C. Werner, and L. Carbognin, "Assessing short- and long-time displacements in the venice coastland by synthetic aperture radar interferometric point target analysis," *J. Geophys. Res.*, vol. 112, no. F1, 2007.

[9] J. Hu, Z. W. Li, X. L. Ding, J. J. Zhu, L. Zhang, and Q. Sun, "Resolving three-dimensional surface displacements from InSAR measurements: A review," *Earth-Science Rev.*, vol. 133, pp. 1–17, Jun. 2014.

[10] L. Ge, C. Rizos, S. Han, and H. Zebker, "Mining subsidence monitoring using the combined InSAR and GPS approach," in *Proc. 10th Int. Symp. Deformation Meas.*, 2001, pp. 1–10.

[11] M. Liao, T. Balz, F. Rocca, and D. Li, "Paradigm changes in surface-motion estimation from SAR: Lessons from 16 years of Sino-European cooperation in the dragon program," *IEEE Geosci. Remote Sens. Mag.*, vol. 8, no. 1, pp. 8–21, Mar. 2020.

[12] L. Wang, K. Deng, H. Fan, and F. Zhou, "Monitoring of large-scale deformation in mining areas using sub-band InSAR and the probability integral fusion method," *Int. J. Remote Sens.*, vol. 40, no. 7, pp. 2602–2622, Apr. 2019.

[13] L. Wang, K. Deng, and M. Zheng, "Research on ground deformation monitoring method in mining areas using the probability integral model fusion D-InSAR, sub-band InSAR and offset-tracking," *Int. J. Appl. Earth Observ. Geoinformation*, vol. 85, Mar. 2020, Art. no. 101981.

[14] D. Liu, Y. Shao, Z. Liu, B. Riedel, A. Sowter, W. Niemeier, and Z. Bian, "Evaluation of InSAR and TomoSAR for monitoring deformations caused by mining in a mountainous area with high resolution satellite-based SAR," *Remote Sens.*, vol. 6, no. 2, pp. 1476–1495, Feb. 2014.

[15] L. Ge, E. Cheng, X. Li, and C. Rizos, "Quantitative subsidence monitoring: The integrated InSAR, GPS and GIS approach," in *Proc. 6th Int. Symp. Satell. Navigat. Technol. Including Mobil Positioning Location Services*, vol. 87, 2003, pp. 1–13.

[16] Z. W. Li, Z. F. Yang, J. J. Zhu, J. Hu, Y. J. Wang, P. X. Li, and G. L. Chen, "Retrieving three-dimensional displacement fields of mining areas from a single InSAR pair," *J. Geodesy*, vol. 89, no. 1, pp. 17–32, Jan. 2015.

[17] X. Diao, K. Wu, D. Hu, L. Li, and D. Zhou, "Combining differential SAR interferometry and the probability integral method for three-dimensional deformation monitoring of mining areas," *Int. J. Remote Sens.*, vol. 37, no. 21, pp. 5196–5212, Nov. 2016.

[18] C. Zhao, Z. Lu, and Q. Zhang, "Time-series deformation monitoring over mining regions with SAR intensity-based offset measurements," *Remote Sens. Lett.*, vol. 4, no. 5, pp. 436–445, May 2013.

[19] H. Fan, X. Gao, J. Yang, K. Deng, and Y. Yu, "Monitoring mining subsidence using a combination of phase-stacking and offset-tracking methods," *Remote Sens.*, vol. 7, no. 7, pp. 9166–9183, Jul. 2015.

[20] J. Huang, K. Deng, H. Fan, and S. Yan, "An improved pixel-tracking method for monitoring mining subsidence," *Remote Sens. Lett.*, vol. 7, no. 8, pp. 731–740, Aug. 2016.

[21] S. Yan, G. Liu, K. Deng, Y. Wang, S. Zhang, and F. Zhao, "Large deformation monitoring over a coal mining region using pixel-tracking method with high-resolution Radarsat-2 imagery," *Remote Sens. Lett.*, vol. 7, no. 3, pp. 219–228, Mar. 2016.

[22] J. Huang, K. Deng, H. Fan, S. Lei, S. Yan, and L. Wang, "An improved adaptive template size pixel-tracking method for monitoring large-gradient mining subsidence," *J. Sensors*, vol. 2017, Sep. 2017, Art. no. 3059159.

[23] Z. Wang, S. Yu, Q. Tao, G. Liu, H. Hao, K. Wang, and C. Zhou, "A method of monitoring three-dimensional ground displacement in mining areas by integrating multiple InSAR methods," *Int. J. Remote Sens.*, vol. 39, no. 4, pp. 1199–1219, Feb. 2018.

[24] M. Zheng, K. Deng, H. Fan, and J. Huang, "Monitoring and analysis of mining 3D deformation by multi-platform SAR images with the probability integral method," *Frontiers Earth Sci.*, vol. 13, no. 1, pp. 169–179, Mar. 2019.

[25] B. Q. Chen and K. Z. Deng, "Integration of D-InSAR technology and PSO-SVR algorithm for time series monitoring and dynamic prediction of coal mining subsidence," *Surv. Rev.*, vol. 46, no. 339, pp. 392–400, Nov. 2014.

[26] Z. Yang, Z. Li, J. Zhu, A. Preusse, H. Yi, J. Hu, G. Feng, and M. Papst, "Retrieving 3-D large displacements of mining areas from a single amplitude pair of SAR using offset tracking," *Remote Sens.*, vol. 9, no. 4, pp. 338–355, 2017.

[27] Z. Yang, Z. Li, J. Zhu, A. Preusse, J. Hu, G. Feng, and M. Papst, "Time-series 3-D mining-induced large displacement modeling and robust estimation from a single-geometry SAR amplitude data set," *IEEE Trans. Geosci. Remote Sens.*, vol. 56, no. 6, pp. 3600–3610, Jun. 2018.

[28] Z. Yang, Z. Li, J. Zhu, A. Preusse, J. Hu, G. Feng, and M. Papst, "High-resolution three-dimensional displacement retrieval of mining areas from a single SAR amplitude pair using the SPIKE algorithm," *IEEE J. Sel. Topics Appl. Earth Observ. Remote Sens.*, vol. 11, no. 10, pp. 3782–3793, Oct. 2018.

[29] Z. Yang, Z. Li, J. Zhu, Y. Wang, and L. Wu, "Use of SAR/InSAR in mining deformation monitoring, parameter inversion, and forward predictions: A review," *IEEE Geosci. Remote Sens. Mag.*, vol. 8, no. 1, pp. 71–90, Mar. 2020.

[30] Z. Yang, Z. Li, J. Zhu, A. Preusse, J. Hu, G. Feng, H. Yi, and M. Papst, "An alternative method for estimating 3-D large displacements of mining areas from a single SAR amplitude pair using offset tracking," *IEEE Trans. Geosci. Remote Sens.*, vol. 56, no. 7, pp. 3645–3656, Jul. 2018.

[31] B. Chen, Z. Li, C. Yu, D. Fairbairn, J. Kang, J. Hu, and L. Liang, "Three-dimensional time-varying large surface displacements in coal exploiting areas revealed through integration of SAR pixel offset measurements and mining subsidence model," *Remote Sens. Environ.*, vol. 240, Apr. 2020, Art. no. 111663.

[32] F. Casu, A. Manconi, A. Pepe, and R. Lanari, "Deformation time-series generation in areas characterized by large displacement dynamics: The SAR amplitude pixel-offset SBAS technique," *IEEE Trans. Geosci. Remote Sens.*, vol. 49, no. 7, pp. 2752–2763, Jul. 2011.
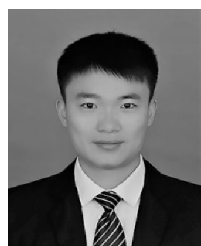
YANG BAI received the B.S. degree in surveying engineering from the PLA Information Engineering University, Zhengzhou, China, in 2011, and the Ph.D. degree in photogrammetry and remote sensing from the China University of Mining and Technology, Xuzhou, China, in 2016.

She is currently working with the College of Environment and Planning, Henan University. Her research interest includes remote sensing image processing and its applications on ecological environment monitoring.

SHAOGANG LEI received the Ph.D. degree in geography information system from the China University of Mining and Technology, Xuzhou, China, in 2009.

He is currently a Full Professor with the School of Environmental Science and Spatial Informatics, China University of Mining and Technology. His research interests include remote sensing of mine environment, UAV remote sensing, and ecology restoration.

JILEI HUANG received the M.S. degree in surveying engineering from the Kunming University of Science and Technology, Kunming, China, in 2014, and the Ph.D. degree in geodesy and surveying engineering from the China University of Mining and Technology, Xuzhou, China, in 2017.

He is currently working with the College of Resources and Environment, Henan University of Economics and Law. His research interests include interferometric synthetic aperture radar and its applications on mining subsidence, mine disaster monitoring, and ecological environment monitoring in mining area.

KAZHONG DENG received the M.S. degree in mine surveying and the Ph.D. degree in mining engineering from the China University of Mining and Technology, Xuzhou, China, in 1986 and 1993, respectively.

He is currently a Full Professor with the School of Environmental Science and Spatial Informatics, China University of Mining and Technology. His research interests include coal mining subsidence, mine disaster monitoring, and spaceborne geodetic technologies, such as GPS and InSAR.

● ● ●